Model for transition from upper to lower bainite

An attempt is made to model the transition from upper to lower bainite in steels, based on the hypothesis that bainitic ferrite grows with a supersaturation of carbon in solid solution. The theory involves a comparison between the time required to reject the excess carbon into the residual austenite by diffusion and the time required to obtain a detectable degree of cementite precipitation in the bainitic ferrite. If the precipitation process is relatively rapid, then it is assumed that lower bainite is obtained. The results are found to be in broad agreement with published experimental data.

MST/1095

M. Takahashi
H. K. D. H. Bhadeshia

 Manuscript received 5 May 1989; in final form 20 July 1989. *The authors are in the Department of Materials Science and Metallurgy, University of Cambridge.*

List of symbols

- B_s bainite start temperature
- c thickness of cementite plate
- D diffusivity of carbon in austenite, $m^2\ s^{-1}$
- $\underline{D}$ weighted average diffusivity of carbon in austenite, $m^2\ s^{-1}$
- D_α diffusivity of carbon in ferrite, $m^2\ s^{-1}$
- f volume fraction of cementite particles
- G_1^* activation free energy of nucleus formation on a dislocation, $J\ mol^{-1}$
- G_2^* activation energy for transfer of atoms across nucleus/matrix interface, $J\ mol^{-1}$
- h Planck's constant, J s
- H_0 hardness of as quenched virgin martensite
- H_F hardness of martensite when all carbon has precipitated, but before onset of recovery or coarsening of cementite particles
- $H\{t\}$ hardness of martensite at time t during tempering
- H_V hardness of martensite
- ΔH_V change in hardness of martensite due to cementite precipitation during tempering
- I nucleation rate per unit volume, $m^{-3}\ s^{-1}$
- k, k_0 rate constants in Avrami type equation
- k_ε, k_p coefficients of ε_1 and Δ in equation of yield strength of martensite
- l radius of cementite plate
- L_s lower bainite start temperature
- M_s martensite start temperature
- n rate constant in Avrami type equation
- N^v number of atoms per unit volume which are on dislocation lines, m^{-3}
- N_V number of cementite particles at completion of precipitation, m^{-3}
- p Péclet number
- Q effective activation energy for cementite precipitation, $J\ mol^{-1}$
- r average cementite particle radius, m
- r_0 average cementite particle radius before onset of Ostwald ripening
- R universal gas constant, $J\ mol^{-1}\ K^{-1}$
- S_1, S_2 functions of p in equation (26)
- t time, s
- t_C time required for carbon concentration in ferrite to decrease to specified level, s
- t_d time required to decarburise plate of bainitic ferrite of thickness w
- t_ε time required to obtain detectable amount of ε carbide in bainitic ferrite
- t_θ time required to obtain detectable amount of cementite precipitation in bainitic ferrite
- T absolute temperature
- T_0' temperature at which parent and product phases of identical composition have same free energy
- v edgewise growth rate of cementite plates, $m\ s^{-1}$
- v_c velocity of flat interface which is controlled by interface kinetics only, $m\ s^{-1}$
- v_θ volume of cementite plate, m^3
- V_θ^e maximum volume fraction of cementite
- $\bar{V}$ partial molar volume fraction of solvent in cementite
- w thickness of plate of bainitic ferrite, m
- $\bar{x}$ average carbon concentration in steel, mole fraction
- $x_{T_0'}$ carbon concentration at T_0' curve, mole fraction
- x^α carbon concentration in ferrite
- $x^{\alpha\gamma}$ carbon concentration in ferrite which is in equilibrium or paraequilibrium with austenite, mole fraction
- x^γ carbon concentration in austenite
- $x^{\gamma\alpha}$ carbon concentration in austenite which is in equilibrium or paraequilibrium with ferrite, mole fraction
- $x^{\alpha\theta}$ carbon concentration in ferrite which is in equilibrium or paraequilibrium with cementite, mole fraction
- $x^{\theta\alpha}$ carbon concentration in cementite which is in equilibrium or paraequilibrium with ferrite, mole fraction
- $x^{\gamma\theta}$ carbon concentration in γ which is in equilibrium or paraequilibrium with cementite, mole fraction
- α_1 one dimensional parabolic thickening rate constant, $m\ s^{-1/2}$
- α_{LB} lower bainite
- α_{UB} upper bainite
- β aspect ratio of cementite plates
- β_0 constant in nucleation function of cementite
- β_1 lengthening rate of cementite plates, $m\ s^{-1}$
- γ austenite
- Γ_D capillarity constant
- Δ average distance between particle and its two or three nearest neighbours
- ε ε carbide
- ε_1 average transverse thickness of martensite cell structure
- η number of cementite particles/unit volume, m^{-3}
- θ cementite
- μ_0 interfacial mobility
- ξ_e extended volume fraction of cementite normalised by its equilibrium volume fraction at reaction temperature V_θ^e
- $\xi\{t\}$ volume fraction of cementite at time t normalised by its equilibrium volume fraction at reaction temperature V_θ^e

ρ dislocation density in ferrite, m^{-2}
σ interfacial free energy per unit area between ferrite and cementite, $J\,m^{-2}$
σ_C solid solution strengthening effect of carbon, $MN\,m^{-2}$
σ_0 intrinsic strength of martensite, $MN\,m^{-2}$
σ_0' residual strength of martensite, $MN\,m^{-2}$
σ_y yield strength of martensite, $MN\,m^{-2}$
$\Delta\sigma_y$ change of yield strength, due to cementite precipitation in initial stages of tempering, $MN\,m^{-2}$
τ incubation period for cementite precipitation, s
ϕ radius of curvature at advancing tip of plate, m
ϕ_c critical radius for growth at which concentration difference in matrix vanishes in absence of interface kinetics, m
Ω_0 dimensionless supersaturation parameter

Introduction

Bainite can be regarded as a non-lamellar mixture of ferrite and carbides, but within this broad description, it is possible to identify two classical morphologies, traditionally called upper and lower bainite (e.g. *see* Ref. 1–4). Lower bainite is usually obtained by transformation at lower temperatures, although both phases can sometimes be found in the same microstructure. Both upper and lower bainite tend to form as aggregates (sheaves) of small platelets or laths (subunits) of ferrite. The essential difference between upper and lower bainite is with respect to the carbide precipitates. In upper bainite, the bainitic ferrite is free of precipitation, any carbides growing from the regions of carbon enriched residual austenite which are trapped between the subunits of ferrite. By contrast lower bainitic ferrite contains a fine dispersion of plate-like carbides (e.g. ε carbide or cementite) within the bainitic ferrite plates.

The transition between upper and lower bainite is generally thought to occur over a narrow range of temperatures. There are circumstances where both phases can form simultaneously during isothermal transformation close to the transition temperature.[5] The first clear indication of the mechanism of the transition emerged from the work of Matas and Hehemann,[6] whose experiments on several steels (containing 0·38–1·0 wt-%C) indicated a narrow transition temperature range centred around 350°C, irrespective of steel composition. They suggested that the difference between upper and lower bainite is related to the kinetics of carbide precipitation from ferrite. In their model, both upper and lower bainite form with a supersaturation of carbon, but with the former, almost all of the excess carbon is rejected into the residual austenite; with lower bainite, carbon precipitates rapidly in the supersaturated ferrite, so that the amount that diffuses into the residual austenite is reduced. The relatively constant transition temperature was explained by suggesting that ε carbide will, for some reason, not precipitate from ferrite at temperatures above ~350°C. The ε carbide was envisaged as a precursor to the formation of cementite.

While the Matas and Hehemann model is intuitively reasonable, their assertion that the transition temperature L_s is constant for all steels is not consistent with other experimental results.[5,7–10] The transition temperature can be as high as 500°C and is found to vary with the carbon concentration. The model also requires the carbide in lower bainite to be ε carbide, which might then convert to cementite on further tempering. Later work has shown that it is possible to obtain lower bainite containing the appropriate cementite particles, without any ε carbide as a precursor.[11] Franetovic and co-workers[12,13] have also reported lower bainite containing η carbide (Fe_2C) in a high silicon cast iron and there is no reason to suppose that precipitation temperature and behaviour of η carbide should be similar to that of ε carbide. It is also difficult to explain why ε carbide should not precipitate from ferrite at temperatures above 350°C.

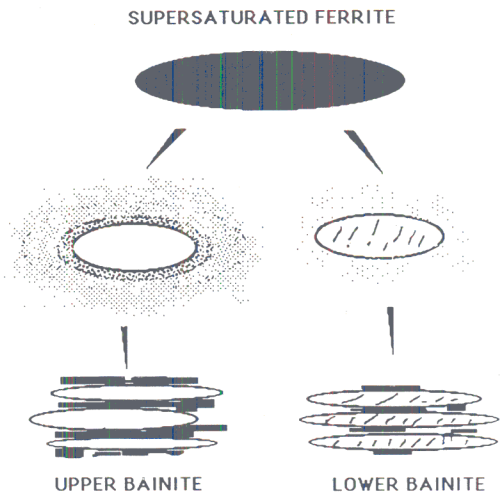

lower bainite is obtained when time required for excess carbon to partition from supersaturated ferrite into residual austenite becomes large relative to time required to precipitate cementite within bainitic ferrite; note that any carbon enrichment of residual austenite may eventually lead to precipitation of further carbides, as illustrated above

1 Schematic illustration of transition from upper to lower bainite

Pickering[5] found that L_s increases initially, then decreases to ~350°C, becoming independent of the carbon concentration beyond ~0·8 wt-%C. His explanation of the transition is essentially the same as that of Matas and Hehemann,[6] that the transition to lower bainite occurs when the rate of carbon diffusion from ferrite is slow, so that the carbides have an opportunity to precipitate. However, the model does not account for any changes in the kinetics of carbide precipitation as a function of carbon concentration. Similar results have been obtained for more heavily alloyed steels, where the peak in the experimental transition curve is found to shift to lower carbon concentrations.[8] Pickering suggested that for high carbon steels (where the transition was claimed to be insensitive to carbon concentration), the cementite precipitates directly from the austenite, as its carbon concentration x^γ exceeds the concentration $x^{\gamma\theta}$ which is given by the extrapolated $\gamma/(\gamma + Fe_3C)$ phase boundary; this does not explain the formation of carbides within the bainitic ferrite.

To summarise, a plausible model for the transition from upper to lower bainite could be constructed from the assumption that there is no fundamental difference in transformation mechanism between these two forms of bainite, if the bainitic ferrite is, when it forms, supersaturated with carbon. The excess carbon may partition eventually into the residual austenite or precipitate from the ferrite in the form of carbides. If the latter process is dominant, then lower bainite is obtained. Upper bainite is obtained only when the carbon partitions relatively rapidly into the residual austenite, before the carbides have an opportunity to precipitate. This is essentially the same as the Matas and Hehemann model,[6] but without the constraint that the transition temperature is limited to a narrow temperature range around 350°C. The model is illustrated schematically in Fig. 1. The purpose of the present work is to test, as far as is possible, the quantitative form of the hypothesis summarised above, and to assess any predictions in the context of available experimental data. The work utilises recent results on the theory for the time required

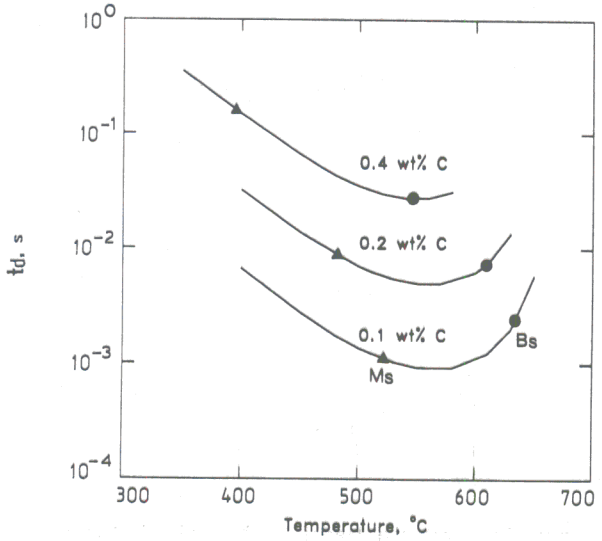

2 Calculated time for decarburisation of supersaturated ferrite plates (of thickness 0·2 μm) in plain carbon steels containing 0·1, 0·2, and 0·4 wt-%C, respectively: calculated martensite start and bainite start temperatures are also indicated

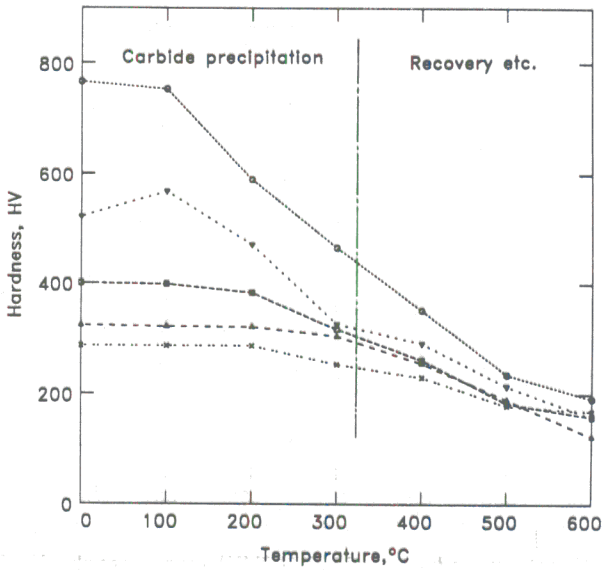

3 Hardness curves (HV0·1) for iron–carbon martensite samples which were tempered for 1 h at temperatures indicated: data left of vertical line largely represent changes due to precipitation of carbides, rather than recovery or coarsening processes (data from Ref. 23)

to decarburise supersaturated ferrite; cementite precipitation kinetics are treated approximately using information from martensite tempering data.

Time required to decarburise supersaturated ferrite

If it is assumed that the diffusivity of carbon in ferrite is very high when compared with that in austenite, and that local paraequilibrium is established during the partitioning of carbon between the austenite and ferrite, then the time required to decarburise a supersaturated bainitic ferrite plate of thickness w is given by[4]

$$t_d = \frac{w^2\pi(\bar{x} - x^{\alpha\gamma})^2}{16\underline{D}(x^{\gamma\alpha} - \bar{x})} \quad \ldots\ldots\ldots\ldots \quad (1)$$

where $\bar{x}$ is the average carbon concentration in the steel as a whole, $x^{\alpha\gamma}$ and $x^{\gamma\alpha}$ are the carbon concentrations in ferrite and austenite respectively, when the two phases are in paraequilibrium. The diffusivity of carbon in austenite is very sensitive to the carbon concentration.[14–17] Hence, when dealing with concentration gradients, it is necessary to consider instead a weighted average diffusivity[18] given by

$$\underline{D} = \int_{\bar{x}}^{x^{\gamma\alpha}} \frac{D\,\mathrm{d}x}{(x^{\gamma\alpha} - \bar{x})} \quad \ldots\ldots\ldots\ldots \quad (2)$$

This procedure is valid strictly for the situation where the concentration profile does not change with time, but is recognised to be a good approximation for non-steady state conditions, as exist during the partitioning of carbon from the supersaturated ferrite. In the present work, the value of D was calculated as discussed in Ref. 19.

The calculated kinetics of partitioning are shown in Fig. 2 for three steels having different carbon concentrations with calculated[20,21] martensite start and bainite start temperatures. For calculations it was assumed that $w =$ 0·2 μm, and this is the approximation used throughout this work. For each steel, the time t_d goes through a minimum as a function of transformation temperature. The minimum occurs because the diffusion coefficient of carbon decreases with temperature (leading to an increase in t_d), while at the same time, the amount of carbon that the austenite can tolerate $x^{\gamma\alpha}$ increases with decreasing temperature; $x^{\gamma\alpha}$ was calculated as in Ref. 22. The decarburisation time also increases as the average carbon concentration of the steel increases; given that an increase in carbon concentration should accelerate the precipitation of carbides in the ferrite, it should lead to an increase in L_s, as reported by Pickering[5] and Llopis and Parker[8] for low carbon concentrations.

Time for precipitation of cementite

Information on the kinetics of the cementite precipitation from supersaturated ferrite is not available in sufficient detail to carry out the first principles calculation of the volume fraction of cementite as a function of time, temperature, and chemical composition. An attempt is made here to derive the overall kinetics of cementite precipitation using published data[23,24] on hardness changes oberved during the initial stages of isothermal tempering of martensite. (Alternative models are presented in the Appendix.)

EMPIRICAL METHOD

When martensite contains an excess concentration of carbon in solid solution, the carbon will tend to precipitate in the form of carbides during tempering. Prolonged annealing can also lead to recovery, recrystallisation, and the coarsening of cementite precipitates. For the present purposes, it is consequently important to focus on the initial stages of tempering, which should represent solely, the effects of precipitation from supersaturated ferrite.

Speich[23] reported that the change in hardness of martensite in plain carbon steels after 1 h of tempering above 320°C, includes significant contributions from recovery, recrystallisation, and coarsening of cementite particles (Fig. 3). Hence, the data representing hardness changes during tempering below 320°C were utilised to obtain a function which expresses the change in the volume fraction

of cementite precipitation as a function of time and temperature. An Avrami type equation[25] was used for the purpose

$$\xi\{t\} = 1 - \exp\{-kt^n\} \quad \ldots\ldots\ldots\ldots \quad (3)$$

where $\xi\{t\}$ is the volume fraction of cementite normalised by its equilibrium volume fraction at the reaction temperature and k and n are rate constants determined from experimental data. It is assumed that $\xi\{t\}$ is related at any time t to the hardness of the martensite $H\{t\}$ as follows

$$\xi\{t\} = \frac{H_0 - H\{t\}}{H_0 - H_F} \quad \ldots\ldots\ldots\ldots \quad (4)$$

H_0 is the hardness of the as quenched virgin martensite, H_F is its hardness when all the carbon has precipitated, but before any significant recovery, recrystallisation, or coarsening has occurred.

Implicit in this relationship is the assumption that the amount of carbon precipitated is linearly related to the change in hardness during the initial stages of tempering.

Using the values of hardness for plain carbon martensite tempered for 1 h at 320°C, reported by Speich,[23] H_F was expressed empirically as a function of the initial hardness and average carbon concentration $\bar{x}$ (mole fraction), as follows

$$H_F = H_0(1 - 1{\cdot}731\bar{x}^{0{\cdot}34}) \quad \ldots\ldots\ldots\ldots \quad (5)$$

This equation is valid for plain carbon steels containing less than 0·4 wt-%C ($\bar{x} < 0{\cdot}0186$), the value of H_F becoming constant thereafter. The hardness H_0 of plain carbon martensite before tempering can also be deduced from the data reported by Speich[23]

$$H_0 = 1267\bar{x}^{0{\cdot}9} + 240 \quad \ldots\ldots\ldots\ldots \quad (6)$$

where the hardness of martensite in pure iron is 240 HV.[24] This equation reflects empirically, the hardness of virgin martensite in plain carbon steels as a function of carbon in solid solution; however, there is evidence to suggest that the effect of carbon tends to saturate, so that H_0 should not exceed a maximum value of about 800 HV irrespective of carbon concentration.[26] Consequently, the maximum value of H_0 permitted in the present analysis is taken to be 800 HV.

INDEPENDENT CALCULATION

There are more elaborate theories available for the change in the strength of low carbon martensite due to the precipitation of cementite, so that the difference $(H_0 - H_F)$ can be evaluated independently from the empirical approach discussed above. The change can be expressed in terms of the decrease in solid solution strengthening as carbon is absorbed during the growth of cementite, and an increase in strength as the cementite particles precipitation harden the martensite. Thus, the yield strength of martensite is expressed as a combination of the intrinsic yield strength, the effect of the dislocation cell structure, and precipitation hardening by cementite[27]

$$\sigma_y = \sigma_0 + k_\varepsilon \varepsilon_1^{-1} + k_p \Delta^{-1} \quad \ldots\ldots\ldots\ldots \quad (7)$$

where σ_0 is the intrinsic strength of martensite, ε_1 is the average transverse thickness of the cell structure, and Δ is the average distance between a particle and its two or three nearest neighbours, given by

$$\Delta = 1{\cdot}18r(2\pi/3f)$$

where r is average particle radius, f is volume fraction of particles, and k_ε and k_p are constants, with $k_p = 0{\cdot}519f^{1/2}$ MN m^{-3}. The value of k_ε is not relevant for the present work since it is the *changes* in hardness before recovery that are of interest.

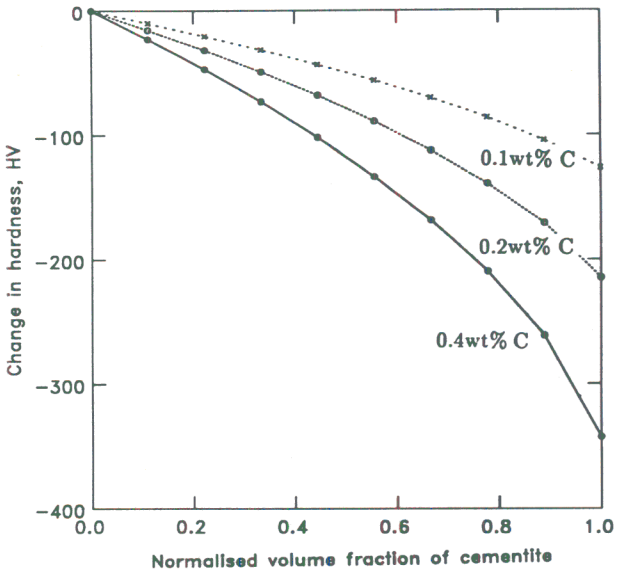

4 Calculated changes in hardness of martensite due to cementite precipitation in 0·1, 0·2, and 0·4 wt-% plain carbon steels: note that horizontal axis represents volume fraction of cementite normalised with respect to its equilibrium volume fraction

The intrinsic strength of martensite can be factorised into the solid solution strengthening effect of carbon σ_C and the residual strength σ_0'

$$\sigma_0 = \sigma_0' + \sigma_C \quad \ldots\ldots\ldots\ldots \quad (8)$$

From the work of Speich and Warlimont[28]

$$\sigma_C = 8 \times 10^3 \bar{x}^{1/2} \quad \ldots\ldots\ldots\ldots \quad (9)$$

Since the hardness relates to the yield strength as follows[28]

$$\sigma_y = 2{\cdot}59H_V - 78{\cdot}20$$

the change in hardness of martensite due to cementite precipitation can be written

$$-\Delta H_V = -0{\cdot}3865\Delta\sigma_y \quad \ldots\ldots\ldots\ldots \quad (10)$$

where $\Delta\sigma_y$ is the change in yield strength due to cementite precipitation in the initial stages of tempering.

Equations to calculate the number of cementite particles and the cementite volume fraction are given below. The calculated hardness changes of martensite in 0·1, 0·2, and 0·4 wt-%C steel, in terms of the decrease in solute carbon and the increase in cementite precipitates, are shown in Fig. 4. Although the relationship between hardness and the amount of the precipitation (thus the decrease in solute carbon) is not linear, the predicted changes in hardness are remarkably consistent with those reported by Speich[23] (Fig. 5).

PARAMETERS FOR AVRAMI EQUATION

The tempering data can now be used to obtain the parameters of the Avrami relationship given in equation (3). For martensite tempered for 1 h, the rate constant k can be calculated using the relationship

$$k = -\ln(1 - \xi\{1\text{ h}\}) \quad (\text{h})^{-n} \quad \ldots\ldots\ldots \quad (11)$$

where $\xi\{1\text{ h}\} = (H_0 - H\{1\text{ h}\})/(H_0 - H_F)$. The calculated values of k for different tempering temperatures for data from Speich[23] can then be used to express k as a function of temperature

$$k = k_0 \exp\left\{-\frac{Q}{RT}\right\} \quad \ldots\ldots\ldots\ldots \quad (12)$$

giving $k_0 = 4{\cdot}07 \times 10^4 \bar{x}^{0{\cdot}635}$ h^{-n}, $Q = 33\,598$ J mol^{-1}.

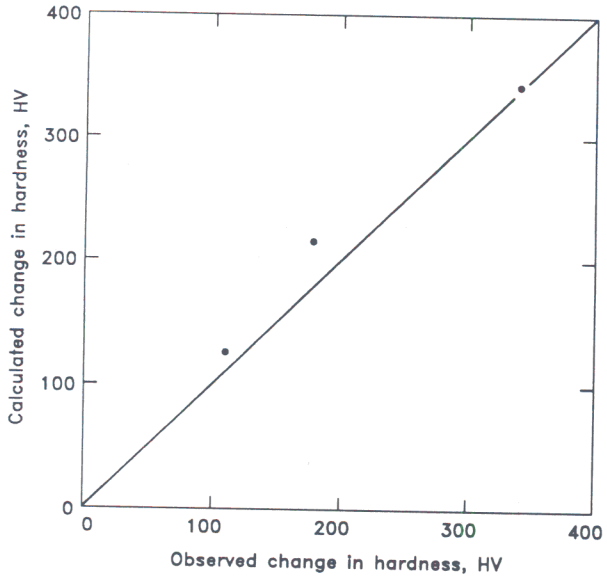

5 Comparison of calculated changes in hardness of plain carbon martensite during tempering, which leads to precipitation of excess carbon in form of cementite, with data reported in Ref. 23

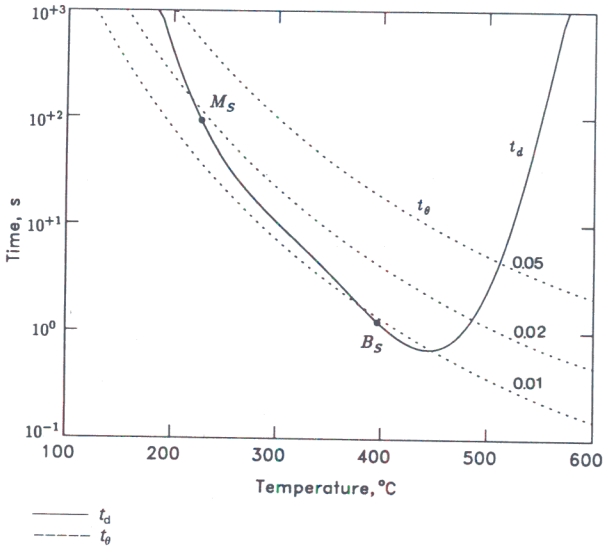

7 Calculated decarburisation time and time required for cementite precipitation, as discussed in text, for Fe–0·43C–2·0Si–3·0Mn (wt-%) alloy: t_θ was calculated for 0·01, 0·02, and 0·05 volume fraction of cementite precipitation

The time exponent n in the Avrami equation can be obtained by plotting log log$[1/(1-\xi\{t\})]$ against log$\{t\}$. The data reported by Speich,[23] which show the changes in hardness during the tempering of martensite in 0·18 and 0·097 wt-%C steels, were used and n was found to be 0·62. It follows that

$$\xi\{t\} = 1 - \exp\{-4{\cdot}07 \times 10^4 \bar{x}^{0{\cdot}635} t^{0{\cdot}62}\} \quad . \ . \ . \ . \quad (13)$$

This equation can be used to estimate the time necessary to obtain a specified degree of transformation as a function of temperature and the carbon concentration of the steel.

The formation of cementite is known to be exceptionally slow in steels containing large amounts of silicon. Bhadeshia and Edmonds[26] measured the change in hardness of martensite by tempering in Fe–0·43C–2·0Si–3·0Mn (wt-%) system at different temperatures. Although their data are not extensive enough to reveal all the constants required in the Avrami equation, k_0 was, for that steel, evaluated by assuming that Q and n are the same as for the plain carbon steels considered previously

$$k = 550 \exp\{-33\,589/RT\} \quad (\text{h})^{-n} \quad . \ . \ . \ . \ . \quad (14)$$

CALIBRATION FOR t_θ

The method used to estimate the upper and lower bainite transition temperature, involves a comparison of the time t_d with the time interval t_θ. If $t_d \ll t_\theta$, then it may be assumed that upper bainite is obtained and vice versa (Fig. 6). Of course, t_θ is a function of ξ, and instead of choosing a detectable value of ξ in an arbitrary way, the value was fixed by comparison with experimental data on L_s. The Fe–0·43C–2·0Si–3·0Mn (wt-%) system is ideal for this purpose since B_s, M_s, and L_s are well characterised.[20] Calculated values of t_d and t_θ (the latter for $\xi = 0{\cdot}01$, 0·02, and 0·05) are plotted, together with B_s, M_s, and L_s in Fig. 7. As expected, the t_d curves exhibit minima, while t_θ was, over the temperature range of interest, found to increase as the reaction temperature decreased. For temperatures below the calculated B_s, where it is possible for bainite to grow, any intersections between the t_d and t_θ curves are of relevance to the location of the transition temperatures. The temperature L_s is defined as the highest temperature at which $t_\theta < t_d$. On comparing the t_θ and t_d curves for the Fe–0·43C–2·0Si–3·0Mn (wt-%) alloy, it was found that the experimental L_s of about 320°C could be

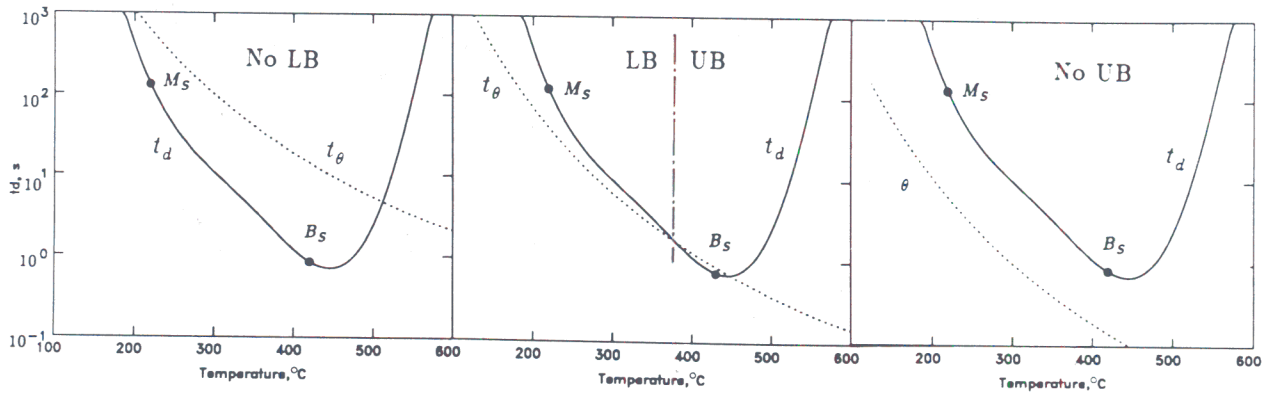

t_d is time required to decarburise plate of ferrite and t_θ is time interval necessary to obtain 'detectable' amount of cementite precipitation in ferrite *a* steel which is incapable of transforming to lower bainite; *b* steel which should, under appropriate transformation conditions, be able to transform to upper or lower bainite; *c* steel in which bainitic transformation always leads to formation of lower bainite

6 Schematic illustration of how differences in relative behaviour of t_d and t_θ curves can lead to various types of transformation behaviour: LB and UB refer to lower and upper bainite, respectively

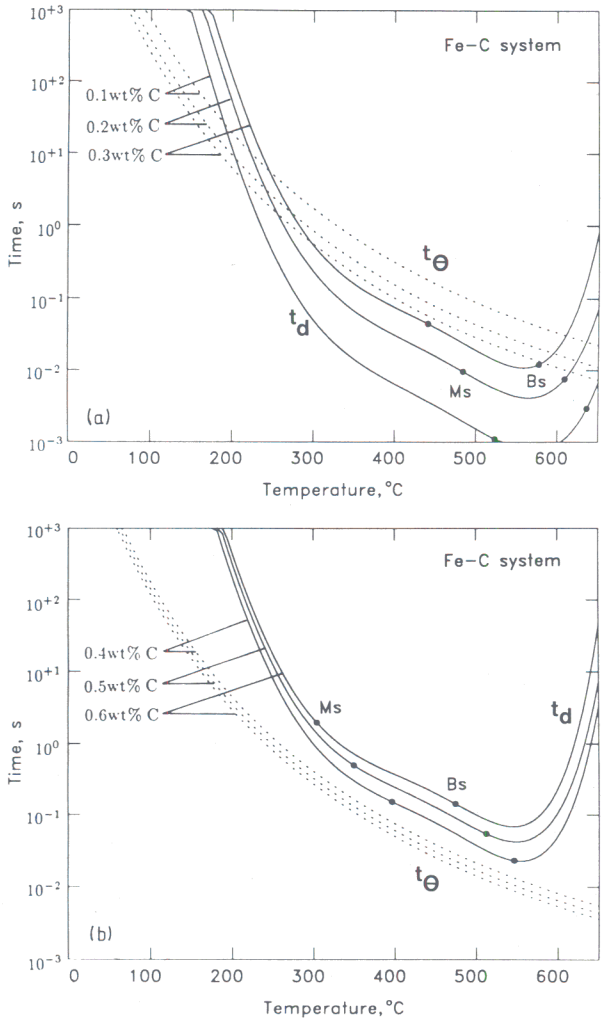

8 Calculated curves of t_d and t_θ for plain carbon steels

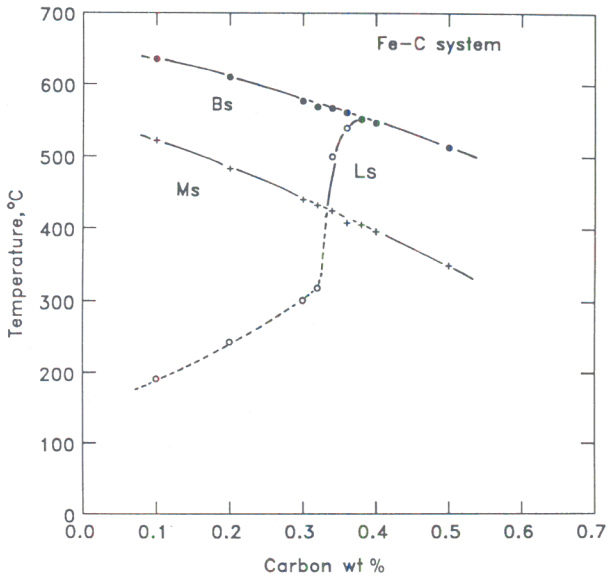

9 Calculated lower bainite transformation start temperatures L_s for plain carbon steels as function of transformation temperature: M_s and B_s are also indicated

predicted fairly accurately if the 'detectable' volume fraction of cementite is set as $\xi = 0{\cdot}01$. Consequently, for all subsequent calculations, L_s is defined by the point where $t_\theta\{\xi = 0{\cdot}01\} < t_d$.

The reason why it is necessary to consider only a very small amount of precipitation (1%) to explain the onset of lower bainite may be that the relationship between the hardness and the amount of carbon atoms used up for the precipitation is not linear (Fig. 3); thus, the calculated 1% precipitation may in reality correspond to a greater degree of precipitation. The time for decarburisation may also be increased by soft impingement of the diffusion fields of neighbouring subunits of bainitic ferrite in a sheaf of bainite. The partitioning of carbon may also be retarded by the precipitation of carbides within the ferrite, since the net flux towards the austenite/ferrite interface would be reduced.

The calculated values of t_d and t_θ for plain carbon steels having carbon concentrations of 0·1, 0·2, 0·3, 0·4, 0·5, and 0·6 wt-% are shown in Fig. 8 as a function of reaction temperature. As expected, the higher the carbon concentration the longer the time required to decarburise the plates. On the other hand, the driving force for cementite precipitation increases with carbon supersaturation, so that t_θ is found to decrease with $\bar{x}$. The calculated M_s and B_s are also plotted in Fig. 8.

The calculated values of L_s are plotted against the carbon content of steels in Fig. 9. According to the calculations, lower bainite should not be observed in plain carbon steels with carbon concentrations less than 0·32 wt-%. Furthermore, only lower bainite (i.e. no upper bainite) should be found in plain C steels of C contents greater than 0·4 wt-%. Steels containing between 0·32 and 0·4 wt-% of carbon should exhibit both upper and lower bainite, depending on the reaction temperatures. Finally, it should be noted that at low temperatures where t_θ and t_d both become very large, the times required for precipitation or redistribution of carbon exceed that to complete transformation, consistent with the fact that untempered martensite can be obtained at temperatures near M_s, with the degree of autotempering of the martensite decreasing as M_s decreases.

Discussion

COMPARISON BETWEEN CALCULATED AND OBSERVED L_s TEMPERATURES

The general behaviour indicated by the calculations for plain carbon steels, is found to be in agreement with that observed experimentally. Some very recent interesting work by Oka and Okamoto[10] (Fig. 10) proves that there is no upper bainite in plain carbon steels containing greater than 0·8 wt-%C; the only bainite observed was classical lower bainite at all temperatures above the M_s. This is consistent with the present calculations.

Ohmori and Honeycombe,[29] in a study of plain carbon steels, showed that during isothermal transformation above the M_s, only upper bainite could be obtained in samples containing less that 0·4 wt-%C (Fig. 11). This is consistent with the calculations presented earlier, although their observation that upper bainite can be obtained in steels having carbon concentrations up to ~0·85 wt-%C is not consistent with the theory, nor with the data reported by Oka and Okamoto.[10] Their diagram additionally indicates a constant L_s of about 350°C, which is also inconsistent with the theory and with the results of Oka and Okamoto. These particular discrepancies and contradictory experimental results cannot be explained at present and further research is required. Although their published diagram[29] is based on experimental data, the actual data points are not presented and it is therefore difficult to assess the validity of some of the boundaries illustrated.

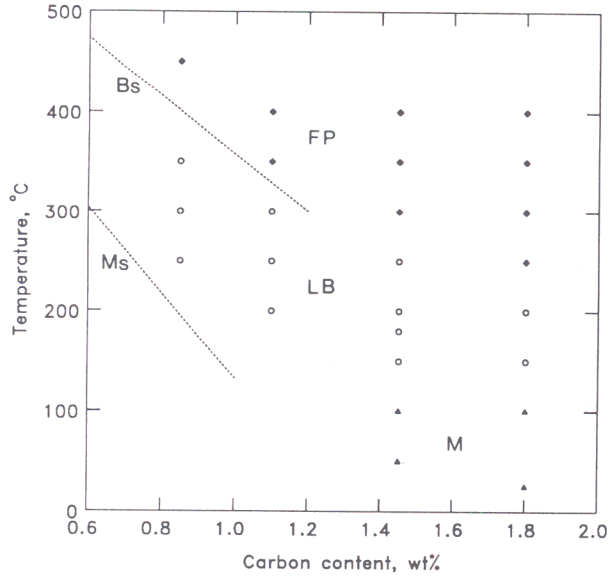

10 Experimental data[10] illustrating temperatures at which fine nodules of pearlite (FP), classical lower bainite (LB), and martensite (M) were obtained by isothermal transformation of plain carbon steels: dotted lines represent bainite start and martensite start temperatures calculated in Refs. 20–22

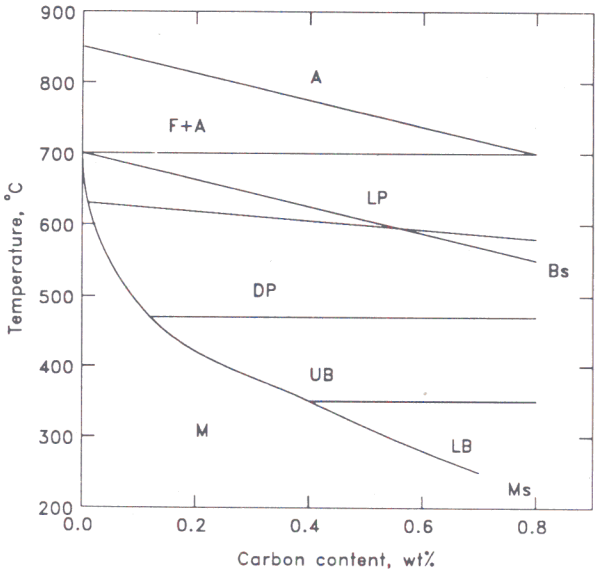

A austenite; F ferrite; LP lamellar pearlite; DP degenerate pearlite; UB upper bainite; LB lower bainite; M martensite; B_S bainite start temperature; M_S martensite start temperature

11 Effect of carbon concentration on temperature range where each microstructure is formed (After Ref. 29)

The change in the transition temperature from upper to lower bainite has also been reported by Pickering[5] and Llopis and Parker[8] for a variety of alloyed steels. Their observations (Fig. 12) show that L_s increases with carbon concentration in the lower carbon region, then goes through a maximum value as the carbon concentration is further increased. After the maximum, L_s is found to stabilise at a constant value. This tendency is consistent with the present calculations, although the reported constant value of L_s at higher carbon concentrations is not. A possible explanation arises from the fact that the calculated[21] values of B_s for the alloys concerned are found to be in very good agreement with values of L_s reported by Pickering[5] for carbon concentrations above 0·4 wt-%. The implication is that the high carbon data become consistent with the work of Oka and Okamoto, if it is assumed that no upper bainite is obtained in those steels, the so called transition temperature corresponding to B_s. Furthermore, considering Pickering's data (excluding some of the other points he plotted from unspecified published research), then the L_s plateau shown in Fig. 12 may simply be an artefact of plotting, since a smooth sloping curve can be fitted through all the high carbon data.

According to the present calculations, only lower bainite is expected in plain C steels containing $>0{\cdot}32$ wt-% of bulk carbon content. However, the calculations are for ferrite plates whose carbon concentration is initially identical to that of bulk alloy, since the model assumes that bainite growth is diffusionless, with carbon redistribution occurring after the growth event. As a consequence of the redistribution, which is expected to be substantial when $t_d < t_\theta$, there is an enrichment in the carbon concentration of residual austenite as the bainite transformation proceeds. Consequently, any bainite which forms from enriched austenite will itself have a higher than bulk concentration of carbon. This leads to the possibility of the transformation beginning with the growth of upper bainite, but with the enriched austenite then decomposing to lower bainite at the later stages of transformation. There is then a real possibilty of obtaining a mixture of upper and lower bainite in steels containing less than 0·32 wt-%C, especially if carbide precipitation from the austenite is relatively sluggish, and therefore does not act to relieve any carbon enrichment in the austenite.

The maximum carbon concentration that can be tolerated in residual austenite before the bainite reaction ceases is expressed approximately by the T'_0 curve.[3,4,22] Therefore, if the carbon concentration in residual austenite at the T'_0 curve (i.e. $x_{T'_0}$) is greater than 0·32 wt-%, lower bainite can be expected to form during the later stages of reaction. However, the formation of cementite from the residual austenite also becomes possible if $x_{T'_0} > x^{\gamma\theta}$, where $x^{\gamma\theta}$ is a point on the $\gamma/(\gamma+\theta)$ phase boundary (calculated as in Refs. 30,31), since the austenite will then be supersaturated with respect to the cementite. The fact that a curve showing

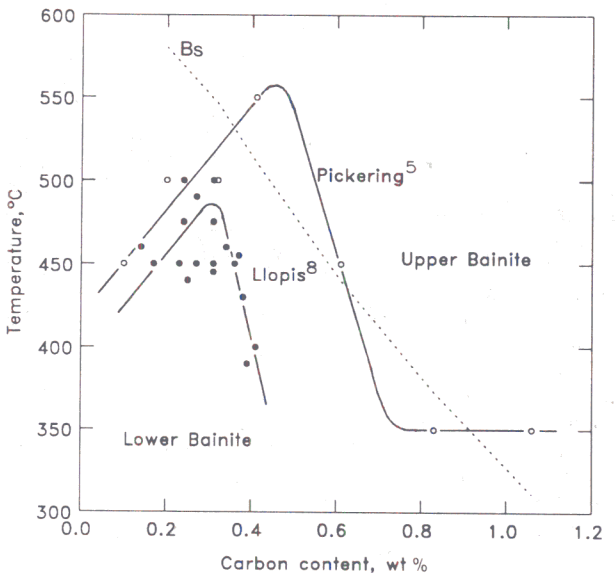

12 Effect of carbon concentration on temperature of change from upper to lower bainite in alloy steels (After Refs. 5 and 8): dotted line represents values of bainite start temperatures calculated as in Refs. 20–22

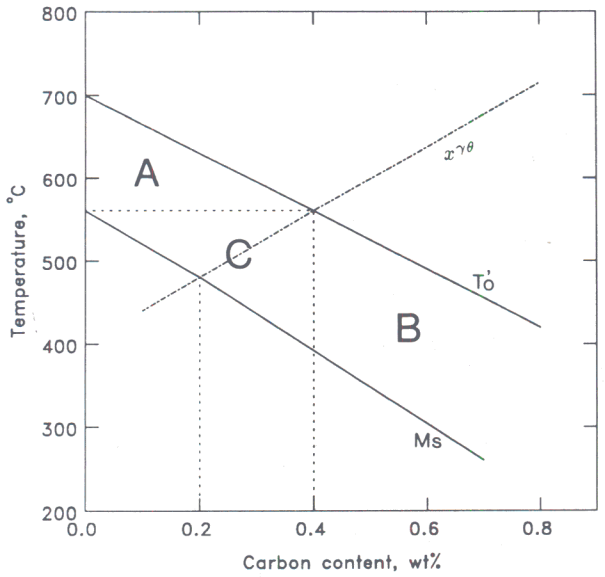

13 Identification of regimes (A, B, C) in which progress of isothermal transformation can lead to changes in nature of transformation product: line marked $x^{\gamma\theta}$ is calculated $\gamma/(\gamma + Fe_3C)$ phase boundary

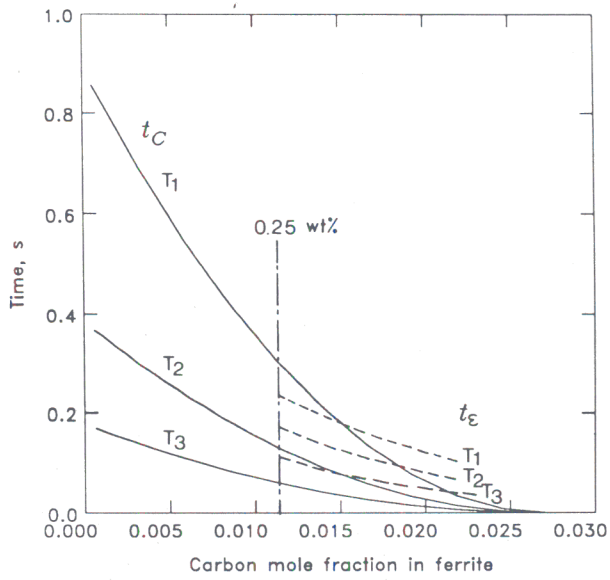

t_ε time to precipitate detectable volume fraction of ε carbide

14 Illustration of possible explanation for transition from lower bainite containing ε carbide to lower bainite containing cementite

the carbon concentration in austenite which is in equilibrium with cementite in plain carbon steels crosses the T_0' curve at 0·4 wt-%C concentration (560°C), leads to the identification of three regimes for bainite on the Fe–C phase diagram (Fig. 13). In steels containing greater than 0·4 wt-% of the initial bulk carbon content (region B), lower bainite is to be expected from the earliest stages of transformation. For steels whose composition lies in region A, lower bainite is expected to be absent during isothermal transformation at all temperatures above M_s, and this behaviour is valid for any stage of transformation, since the austenite cannot be supersaturated with cementite as far as regime A is concerned. The behaviour in the region marked C should be more complex. The residual austenite for these steels (region C) may at some stage of transformation contain enough carbon to precipitate cementite. If the kinetics of cementite precipitation from austenite are rapid, then lower bainite may not be obtained in steels having an average carbon concentration less than 0·32 wt-%, but otherwise, a mixed microstructure of upper and lower bainite might arise.

COMPARISON WITH TEMPERING OF MARTENSITE

In the present model for the upper to lower bainite transition, the microstructure of lower bainite in effect arises from the 'autotempering' of supersaturated plates of bainitic ferrite. The lower bainite should consequently exhibit many of the characteristics of tempered martensite. When high carbon martensite is tempered, the first carbide to form is usually a transition carbide such as ε carbide, which is replaced eventually by the thermodynamically more stable cementite. Similarly, when lower bainite forms in high carbon steels, ε carbide forms first, and transforms subsequently into cementite during prolonged holding at the isothermal transformation temperature.[6]

The chances of obtaining ε carbide (instead of cementite) in lower bainite increase as the transformation temperature is reduced for the same steel (*see* Table II of Ref. 6). As the transformation temperature decreases, and the time required to decarburise a supersaturated plate of bainite increases, a high carbon concentration can persist in the ferritic matrix for a time period long enough to allow the formation of ε carbide, which does not form if the carbon concentration is less than about 0·25 wt-%.[32] This effect also explains the result that a medium carbon Fe–0·43C–3Mn–2Si (wt-%) steel transforms to lower bainite containing cementite particles,[33] although when quenched to martensite it gives ε carbide on tempering.[26] Some of the carbon is in the former case, lost to the austenite by diffusion, thereby preventing the formation of ε carbide.

The ideas discussed here can in principle be predicted using the present model. Figure 14 illustrates calculations for a Fe–0·6 wt-%C alloy, for transformation temperatures where only lower bainite is obtained. The continuous curves represent the time required for the carbon concentration in the bainitic ferrite to drop to a specified level, and the vertical line represents the time t_C taken for this concentration to reach 0·25 wt-%, the level below which ε carbide should not form.[32] The bainitic ferrite is assumed to have an initial carbon concentration of 0·6 wt-%. The curves are calculated using equation (1), but by replacing $x^{\alpha\gamma}$ by x^{α}, which represents the amount of carbon in the bainitic ferrite at any instant of time, with $x^{\alpha\gamma} \leqslant x^{\alpha} \leqslant \bar{x}$. The dashed curves are schematic, and represent the time t_ε; there is as yet no theory which can predict these curves, nor are there suitable experimental data which can be used to estimate the curves empirically. Although the curves are schematic, their form is based on the corresponding curves for cementite, as used in the earlier analysis. If $t_\varepsilon < t_C$, then the lower bainite should contain ε carbide rather than cementite and vice versa. It is evident that it is possible to envisage circumstances where a lowering of the transformation temperature can lead to a transition from lower bainite containing cementite to lower bainite containing ε carbide. A similar diagram could be used to rationalise the observation that in a medium carbon steel, the lower bainite is found to contain cementite, while the tempering of martensite in the same steel leads to ε carbide formation.

OTHER DIFFERENCES BETWEEN UPPER AND LOWER BAINITE

The fact that lower bainite forms at a higher undercooling below B_s when compared with upper bainite has other implications. Subunit growth during the bainite transformation ceases when the interface is blocked by plastic accommodation induced defects.[34] For a given defect density, lower bainite subunits should be longer than those

of upper bainite, since the driving force for transformation increases with undercooling. At lower transformation temperatures the matrix is able to support higher strains without plastic deformation so that the defect density *in the matrix itself* would be lower. Step quenching experiments in which an alloy is first partially transformed to lower bainite and then up-quenched into the upper bainite transformation range are consistent with this, since they show that the growth of lower bainite ceases following the up-quench.[35] This also appears to be the case when specimens partially transformed to lower bainite experience an increase in temperature within the lower bainite transformation range.[36]

Conclusions

A model, based on an idea of Matas and Hehemann,[6] has been developed to enable the estimation of the temperature at which the upper bainite reaction gives way to the formation of lower bainite. The model involves a comparison between the times required to decarburise supersaturated ferrite plates with the time required to precipitate cementite within the plates. If the decarburisation process dominates, upper bainite is predicted, whereas relatively rapid carbide precipitation within the ferrite leads to the formation of lower bainite.

Some of the predictions of the theory are in agreement with reported experimental data. Consistent with the results of Ohmori and Honeycombe,[29] it is found that lower bainite cannot form in plain carbon steels containing less that ~0·3 wt-%C. Upper bainite is predicted to be absent in plain carbon steels containing greater than 0·4 wt-%C; this is in agreement with the results of Oka and Okamoto,[10] although contradictory results have been reported by Ohmori and Honeycombe,[29] who were able to obtain both upper and lower bainite in high carbon Fe–C alloys. The maximum in the curve of transition temperature versus carbon concentration, reported by Pickering[5] and Llopis and Parker[8] is also consistent with the theory.

To summarise, more experimental work is required to verify some of the detailed predictions of the model, and to resolve some of the discrepancies between experimental data reported in the literature. More work is also required from a theoretical point of view, to develop fully the kinetics of cementite precipitation from supersaturated ferrite, and to couple the processes of cementite precipitation with the simultaneous redistribution of carbon into the residual austenite. For the present, the current model seems to provide a rational basis for the transition temperature.

Acknowledgments

The authors are grateful to the Nippon Steel Corporation for funding this research and to Professor D. Hull for the provision of laboratory facilities at the University of Cambridge.

References

1. R. F. MEHL: 'Hardenability of alloy steels', 1; 1939, Metals Park, OH, ASM.
2. R. F. HEHEMANN: 'Phase transformations', 397–432; 1970, Metals Park, OH, ASM.
3. J. W. CHRISTIAN and D. V. EDMONDS: 'Phase transformations in ferrous alloys', (ed. A. R. Marder and J. I. Goldstein) 293–326; 1984, Metals Park, OH, ASM.
4. H. K. D. H. BHADESHIA: 'Phase transformations '87', (ed. G. W. Lorimer), 309–314; 1988, London, The Institute of Metals.
5. F. B. PICKERING: 'Transformation and hardenabilty in steels', 109–132; 1967, Ann Arbor, MI, Climax Molybdenum.
6. S. J. MATAS and R. F. HEHEMANN: *Trans. AIME*, 1961, **221**, 179–185.
7. S. MATSUDA: *Tetsu-to-Hagané* (*J. Iron Steel Inst. Jpn*), 1970, **56**, 1428.
8. A. M. LLOPIS, referred to in E. R. Parker: *Metall. Trans.*, 1977, **8A**, 1025–1042.
9. H. K. D. H. BHADESHIA: *Acta Metall.*, 1980, **28**, 1103–1114.
10. M. OKA and H. OKAMOTO: Proc. Int. Conf. 'Martensitic transformations '86', 271–275; 1986, Tokyo, The Japan Institute of Metals.
11. H. K. D. H. BHADESHIA and D. V. EDMONDS: *Met. Sci.*, 1979, **13**, 325–334.
12. V. FRANETOVIC, A. K. SACHDEV, and E. F. RYNTZ: *Metallography*, 1987, **20**, 15–36.
13. V. FRANETOVIC, M. M. SHEC, and E. F. RYNTZ: *Mater. Sci. Eng.*, 1987, **96**, 231–245.
14. R. P. SMITH: *Acta Metall.*, 1953, **1**, 578.
15. C. WELLS, W. BATZ, and R. F. MEHL: *Trans. AIME*, 1950, **188**, 533.
16. R. H. SILLER and R. B. MCLELLAN: *Trans. AIME*, 1969, **245**, 697.
17. R. H. SILLER and R. B. MCLELLAN: *Metall. Trans.*, 1970, **1**, 985.
18. R. TRIVEDI and G. M. POUND: *J. Appl. Phys.*, 1967, **38**, 3569–3576.
19. H. K. D. H. BHADESHIA: *Met. Sci.*, 1981, **15**, 477–479.
20. H. K. D. H. BHADESHIA and D. V. EDMONDS: *Acta Metall.*, 1980, **28**, 1265–1273.
21. H. K. D. H. BHADESHIA: *Met. Sci.*, 1981, **15**, 178–180.
22. H. K. D. H. BHADESHIA: *Acta Metall.*, 1981, **29**, 1117–1130.
23. G. R. SPEICH: *Trans. AIME*, 1969, **245**, 2553–2564.
24. W. C. LESLIE: 'The physical metallurgy of steels', 211–269; 1981, New York, McGraw-Hill.
25. J. W. CHRISTIAN: 'Theory of transformations in metals and alloys, 2 edn, Part 1; 1975, Oxford, Pergamon Press.
26. H. K. D. H. BHADESHIA and D. V. EDMONDS: *Met. Sci.*, 1983, **17**, 411–419.
27. J. DAIGNE, M. GUTTMANN, and J. P. NAYLOR: *Mater. Sci. Eng.*, 1982, **56**, 1–10.
28. G. R. SPEICH and H. WARLIMONT: *J. Iron Steel Inst.*, April 1968, 385–392.
29. Y. OHMORI and R. W. K. HONEYCOMBE: *Trans. Iron Steel Inst. Jpn*, 1971, **11**, 1160–1164.
30. C. ZENER: *Trans. AIME*, 1969, **169**, 513–534.
31. W. A. WEST: *Trans. AIME*, 1969, **169**, 535–549.
32. C. S. ROBERTS, B. L. AVERBACH, and M. COHEN: *Trans. ASM*, 1957, **45**, 576.
33. H. K. D. H. BHADESHIA and D. V. EDMONDS: *Met. Sci.*, 1979, **13**, 325–334.
34. H. K. D. H. BHADESHIA and D. V. EDMONDS: *Metall. Trans.*, 1979, **10A**, 895–907.
35. R. H. GOODENOW and R. F. HEHEMANN: *Trans. AIME*, 1965, **233**, 1777.
36. J. S. WHITE and W. OWEN: *J. Iron Steel Inst.*, 1961, **197**, 241–243.

Appendix

Further modelling of kinetics of cementite precipitation in ferrite

In this section, alternative models for the kinetics of cementite precipitation in ferrite are considered, with the aim of examining the posibility of more fundamental theory compared with the rather empirical martensite tempering data based methods used above. Such models could be useful in taking account of alloying element effects on the kinetics of cementite precipitation from supersaturated ferrite, and hence permit an easy extension of the transition work to alloy steels.

DIFFUSION CONTROLLED FORMATION OF CEMENTITE 'ALLOTRIOMORPHS'

It is assumed here that the growth of cementite platelets is controlled by the diffusion of carbon in the supersaturated ferrite and that it involves the one dimensional advance of interfaces parallel to the habit plane of each cementite particle. A one dimensional parabolic thickening rate constant for this process can be calculated using the following equation[25]

$$\frac{\bar{x}-x^{\alpha\theta}}{x^{\theta\alpha}-x^{\alpha\theta}}=\left(\frac{\pi}{4D_\alpha}\right)^{1/2}\alpha_1\exp\left\{\frac{\alpha_1^2}{4D_\alpha}\right\}\left[1-\mathrm{erf}\left\{\frac{\alpha_1}{4D_\alpha}\right\}\right] \quad (15)$$

where $x^{\theta\alpha}$ and $x^{\alpha\theta}$ are equilibrium carbon concentrations in cementite and ferrite respectively, at the interface between cementite and ferrite, and D_α is the diffusion coefficient of carbon in ferrite.[37]

The lengthening rate of the 'allotriomorphs' of cementite is correspondingly given by a rate constant which is taken to be $\beta_1 \approx 3\alpha_1$; this seems somewhat arbitrary, but gives a similar aspect ratio to that obtained for allotriomorphic ferrite.[38] The volume of a cementite plate is then given approximately by

$$v_\theta=(\alpha_1 t^{1/2})(\beta_1 t^{1/2})(\beta_1 t^{1/2}) = 9\alpha_1^3 t^{3/2} \quad (16)$$

Venugopalan and Kirkaldy[39] reported the average grain size of cementite (in μm) before the onset of the Ostwald ripening, as a function of tempering temperature T of martensite

$$r_0^3=(2{\cdot}26-6{\cdot}4\times10^{-3}T+4{\cdot}6\times10^{-6}T^2)f\times10^{-3} \quad (17)$$

The number of cementic particles per unit volume can therefore be written as

$$\eta=\frac{V_\theta^e}{\frac{4}{3}\pi r_0^3} \quad (18)$$

where V_θ^e, the maximum volume fraction of cementite obtained at the temperature concerned, can be calculated from the initial carbon concentration in the ferrite $\bar{x}$ by $V_\theta^e \approx 1{\cdot}0065(4\bar{x}/(1-4\bar{x}))$, taking account of the difference in ferrite and cementite densities in respect of the unit cell.

Assuming now, that there is initially a number η of sites available for the growth of cementite, and that no new sites are formed subsequently, the precipitation process can be described simply in terms of the growth of cementite. Thus, using the extended volume method of Avrami to take account of impingement between growing particles, the volume fraction of cementite normalised by the maximum volume fraction V_θ^e is expressed by

$$\xi=1-\exp\{-\xi_e\} \quad (19)$$

where ξ_e is an extended fraction given by

$$\xi_e=9\eta\alpha_1^3 t^{3/2}/V_\theta^e \quad (20)$$

For cases where it may not be justified to start the transformation from a fixed number of growth centres, it is necessary to have some type of nucleation rate function. If it is assumed that nucleation always occurs heterogeneously on dislocations, the nucleation rate per unit volume on dislocations can be written as follows[25,40]

$$I=(N^v)^{1/3}\rho\frac{RT}{h}\exp\left\{-\frac{G_1^*+G_2^*}{RT}\right\} \quad (21)$$

where h is the Planck constant, N^v the number of atoms per unit volume which are on dislocation lines, G_1^* the activation free energy of nucleus formation on a dislocation, G_2^* the activation energy for the transfer of atoms across the nucleus/matrix interface, and ρ the dislocation density. Therefore, the volume fraction of cementite normalised by the maximum volume fraction of cementite is in these circumstances expressed by

$$\xi\{t\}=1-\exp\{-\xi_e\}$$

with

$$\xi_e=\frac{1}{V_\theta^e}I(9\alpha_1^3)\int_0^t(t-\tau)^{3/2}\,\mathrm{d}\tau=\frac{18}{5}\frac{I\alpha_1^3}{V_\theta^e}t^{5/2} \quad (22)$$

where τ is the incubation period.

The activation energy for nucleation should decrease as the inverse square of the driving force for nucleation of cementite from ferrite

$$G_1^* \propto (G^{\theta\alpha})^{-2} \quad (23)$$

so that G_1^* should tend to become small relative to G_2^* at high carbon supersaturations. In such circumstances, G_1^* may be ignored and the nucleation rate may be expected to decrease with undercooling. This is consistent with the data from the empirical analysis discussed above, where it is found that t_θ increases monotonically with a decrease in temperature, rather than showing a C-curve behaviour. Consequently, it seems justified to ignore the G_1^* term for the present analysis, where it is assumed that $G_1^* \ll G_2^*$. The value of G_2^* is not known, but the activation energy for the self-diffusion in ferromagnetic iron[41] is 240 kJ mol^{-1} and since the α/θ interface has a relatively high energy, G_2^* is expected to be less than 240 kJ mol^{-1}. To 'derive' its value, an attempt was made to match the values of η obtained as discussed above, with the number of particles per unit volume, to be expected using the nucleation function in equation (21).

Assuming that the dislocations all lie along $\langle 111\rangle$ directions

$$N^v=\rho/(\tfrac{\sqrt{3}}{2}\times 2{\cdot}8664\times10^{-10})$$

The dislocation density in bainitic ferrite formed at different temperatures has been measured by Smith[42] and Fondekar *et al.*[43] Because these data alone are not adequate to obtain an expression of the dislocation density (in m^{-2}) as a function of the reaction temperature T, similar data for martensite, reported by Kehoe and Kelly,[44] were included in the analysis, to yield the following empirical relationship for the dislocation density in ferrite (Fig. 15)

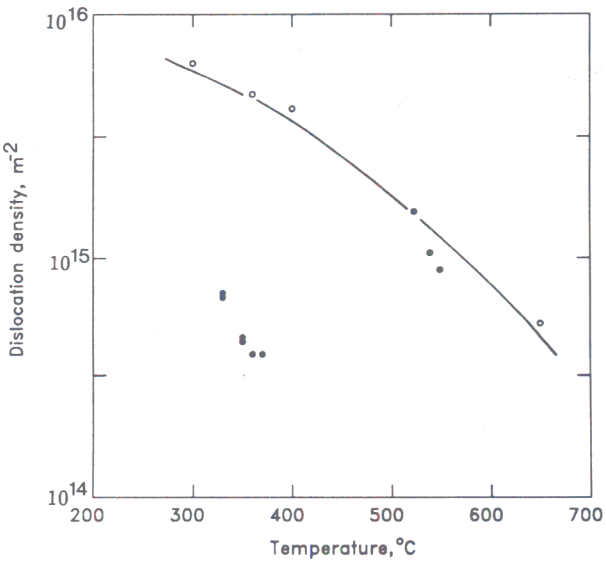

15 Changes in dislocation density of bainitic ferrite (open circles) and martensite (solid circles) as function of reaction temperature: cluster of points that lie below curve are from Ref. 45, other data are from Refs. 42–44

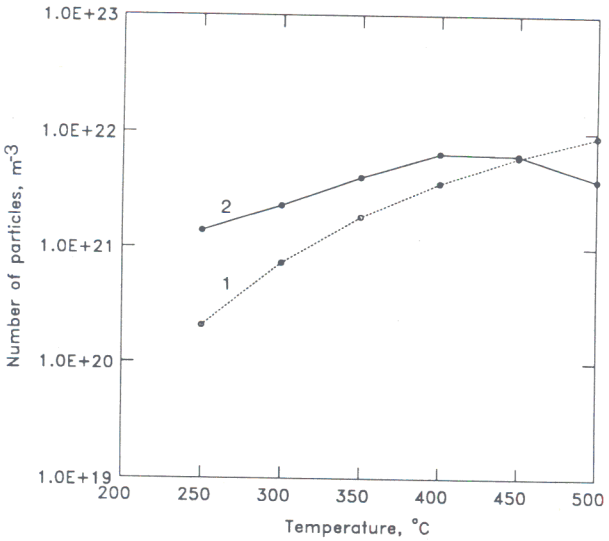

16 Calculated number of cementite particles at completion of precipitation N_V (curve 1) compared with values of η (curve 2) estimated from empirical data of Ref. 39

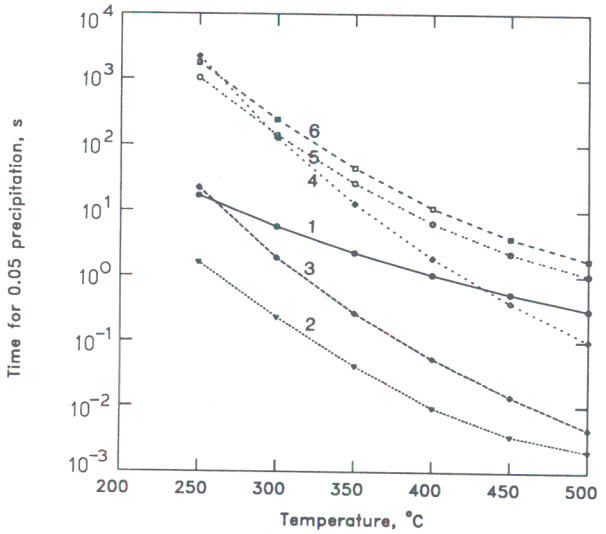

17 Time for ξ = 0·05 cementite precipitation calculated from empirical method (curve 1), parabolic growth model (curve 2), nucleation and parabolic growth model with $G_2^* = 190$ kJ mol^{-1} (curve 3) and with $G_2^* = 240$ kJ mol^{-1} (curve 4), and plate growth model with aspect ratio of 3 (curve 5) and 15 (curve 6) discussed in text, as function of reaction temperature

$$\log \rho = 9{\cdot}28480 + \frac{6880{\cdot}73}{T} - \frac{1\,780\,360}{T^2} \quad \ldots\ldots (24)$$

For martensite, the transformation temperature was taken to be the M_s. Although dislocation densities of martensite measured by Norstöm[45] are also plotted in the figure, those data were not used in deriving the above expression because of uncertainties in the method used to assess the thickness of the thin foil samples used. The curve plotted in Fig. 15 does not therefore take account of these data.

To find the most appropriate value of G_2^*, the number of particles per unit volume at the completion of precipitation was calculated as follows

$$N_V = \int_0^\infty I[1 - \xi\{t\}]\, dt \quad \ldots\ldots\ldots (25)$$

and Fig. 16 shows that a reasonable fit with the empirical data of Venugopalan and Kirkaldy[39] could be obtained by setting $G_2^* = 190$ kJ mol^{-1}. This is the value used in all subsequent calculations.

Another possibility of the calculation of the volume fraction of cementite is based on the theory of diffusion controlled growth of plate shaped particles.[46] The edgewise growth of a precipitate plate from a matrix which is initially at a uniform solute concentration $\bar{x}$, can be obtained from the following equation

$$\Omega_0 = (\pi p)^{1/2} e^p \operatorname{erfc} \sqrt{p}\left[1 + \frac{v}{v_c}\Omega_0 S_1 p + \frac{\phi_c}{\phi}\Omega_0 S_2\, p\right] \quad \ldots\ldots\ldots (26)$$

where v_c is the velocity of a flat interface, controlled by interface kinetics only, ϕ is the radius of curvature at the advancing tip of the plate, ϕ_c is the critical radius for growth at which the concentration difference in the matrix vanishes in absence of the interface kinetics, and v is the edgewise growth rate of the plate,

$$p = \frac{v\phi}{2D_\alpha}$$

$$\phi_c = \frac{x^{\alpha\theta}\Gamma_D}{x^{\alpha\theta} - \bar{x}}$$

$$v_c = \mu_0(x^{\alpha\theta} - \bar{x})$$

$$\Omega_0 = \frac{x^{\alpha\gamma} - \bar{x}}{x^{\alpha\gamma} - x^{\theta\alpha}}$$

The functions S_1 and S_2 have been presented graphically in Ref. 46. The capillarity constant is given by

$$\Gamma_D = \sigma\bar{v}_\theta/(x^{\alpha\theta} - \bar{x})RT$$

where σ is the α/θ interfacial free energy per unit area and $\bar{v}_\theta$ is the molar volume of cementite.

If a disc shape is assumed for a cementite plate (height c, radius l), the volume per cementite plate is

$$v_\theta = \pi l^2 c = \frac{\pi}{\beta} l^3 = \frac{\pi}{\beta}(vt)^3 \quad \ldots\ldots\ldots (27)$$

where β is an aspect ratio of cementite plates. Therefore, using the extended volume method of Avrami, the volume fraction of cementite normalised by the maximum volume fraction of cementite is found to be

$$\xi\{t\} = 1 - \exp\{-\xi_e\} \quad \ldots\ldots\ldots (28)$$

where

$$\xi_e = \eta\frac{\pi}{\beta}(vt)^3/V_\theta^e \quad \ldots\ldots\ldots (29)$$

In Fig. 17, the calculated times required for $\xi = 0{\cdot}05$ of cementite precipitation in an Fe–0·4C (wt-%) alloy in terms of only the parabolic growth, the combination of nucleation and parabolic growth, and plate growth are compared with the calculated times using the empirical methods used above. The calculations used $\sigma = 0{\cdot}7$ J m^{-2} (Ref. 47), $x^{\theta\alpha} = 0{\cdot}25$, and the equilibrium carbon concentration in ferrite as presented in Ref. 48. The aspect ratio in the plate growth model is assumed to be either $\beta = 3$, which is consistent with the parabolic growth model, or $\beta = 15$, which is as observed approximately in Fe–0·43C–2·0Si–3·0Mn (wt-%).

It is evident that the models based on parabolic thickening both indicate much faster transformation kinetics relative to the empirical results, although the result from the nucleation and growth model approaches the empirical result at lower temperatures. The plate growth model, while differing in an absolute sense from the empirical data, gives a similar trend as a function of temperature. It could in principle be adapted (for example, by reducing the number of nucleation sites available per

unit length of dislocation line) to give close agreement with the experimental data. An appropriate selection of the nucleation function for cementite precipitation, and the use of the plate growth theory could, therefore, give closer agreement with the empirical result and allow the estimation of the lower bainite transformation temperature in alloyed steels as well as in plain carbon steels. However, it is essential to investigate the initial stages of the cementite precipitation in detail before any further modifications to the theory for the transition. Note also that the models ignore any precursor reactions such as the precipitation of ε carbide, which may influence the overall kinetics of cementite formation.

References

37. R. B. McLELLAN, M. L. RUDEE, and T. ISHIBACHI: *Trans. AIME*, 1965, **233**, 1938.
38. J. R. BRADLEY and H. I. AARONSON: *Metall. Trans.*, 1977, **8A**, 317.
39. D. VENUGOPALAN and J. S. KIRKALDY: 'Hardenability concept with applications to steel', (ed. D. V. Doane and J. S. Kirkaldy), 249–268; 1978, Warrendale, PA, The Metallurgical Society of AIME.
40. J. W. CAHN: *Acta Metall.*, 1956, **4**, 572.
41. J. FRIDBERG, L.-E. TÖRNDAHL, and M. HILLERT: *Jernkontorets Ann.*, 1969, **153**, 263–276.
42. G. M. SMITH: PhD thesis, University of Cambridge, 1984.
43. M. K. FONDEKAR, A. M. RAO, and A. K. MALLIK: *Metall. Trans.*, 1970, **1**, 885–890.
44. M. KEHOE and P. W. KELLY: *Scr. Metall.*, 1970, **4**, 473–476.
45. L.-A. NORSTRÖM: *Scand. J. Metall.*, 1976, **5**, 159–165.
46. R. TRIVEDI: *Metall. Trans.*, 1970, **1**, 921–927.
47. J. J. KRAMER, G. M. POUND, and R. F. MEHL: *Acta Metall.*, 1958, **6**, 763–771.
48. H. K. D. H. BHADESHIA: *Met. Sci.*, 1982, **16**, 167–169.